

Attention Deficit Hyperactivity Disorder identification: FMRI data analyzed with CNN and seed-based approach

Anika Siamin Oyshi^a, Mohammad Hasan^a, Md. Khabir Uddin Ahamed^a, Md. Sydur Rahman^a, Md. Mahfuzul Haque^b, Mahmudul Alam^{a,*}

^a Department of Computer Science and Engineering, Jamalpur Science and Technology University, Jamalpur-2012, Bangladesh

^b Department of Electrical and Electronic Engineering, Jamalpur Science and Technology University, Jamalpur-2012, Bangladesh

ARTICLE INFO

Keywords:

Attention Deficit Hyperactivity Disorder (ADHD)
Functional Magnetic Resonance Imaging (fMRI)
Default Mode Network (DMN)
Seed-based correlation technique
Convolutional Neural Network (CNN)
Independent Component Analysis (ICA)

ABSTRACT

Attention Deficit Hyperactivity Disorder (ADHD) is a prevalent mental disorder affecting both adults and children, frequently leading to academic difficulties. This study aims to improve the diagnosis of ADHD in children by using resting-state Functional Magnetic Resonance Imaging (fMRI) data. The method uses seed coherence to identify functional connections between specific seed areas and all brain voxels, focusing on Default Mode Network (DMN) regions pertinent to the diagnosis of ADHD. Convolutional Neural Networks (CNNs) are utilized in classification tasks because of their capacity to learn intricate spatial hierarchies. The research utilizes fMRI scans from the ADHDX 200 - Global Competitive dataset, comprising 776 subjects from three prominent data centers. The methodology entails data preparation, feature extraction via seed-based correlation, and classification with Convolutional Neural Networks (CNNs). Three classifiers were assessed: a Neural Network (Keras Sequential Model), a Support Vector Machine (SVM), and a Random Forest Classifier. The optimal outcome was achieved by the neural network, which harmonized precision, recall, and F1 scores, attaining an accuracy of 97 %. The SVM demonstrated considerable accuracy at 83 %, however the Random Forest Classifier exhibited a mere 50 % accuracy, underscoring the necessity for enhancement. These results underscore the merits and shortcomings of each classifier and offer suggestions for enhancement. The paper highlights the significance of Neural Networks for attaining precise and equitable forecasts, proposes enhancements for the Support Vector Machine, and stresses the imperative of optimizing the Random Forest Classifier. This study enhances ADHD diagnosis by methodically employing neuroimaging techniques and assessing several classifiers, leading to a reliable diagnostic system.

1. Introduction

Attention Deficit Hyperactivity Disorder (ADHD) is a prevalent behavioral condition characterized by inattention, hyperactivity, and impulsivity, with a much higher prevalence than in the general population [1,2]. ADHD is projected to impact 7 % of the global population, encompassing around 6.4 million children aged 7 to 14 in the United States. This neurodevelopmental condition, typically diagnosed in early childhood, significantly affects the lives of people impacted, with a prevalence rate of 5–10 % and resulting in long-term deficits [3,4]. The persistent aspect of ADHD is apparent, as symptoms frequently extend into adulthood, resulting in significant repercussions if inadequately addressed [3,4]. Although hyperactivity may be associated with beneficial characteristics such as inventiveness and curiosity, individuals

with ADHD frequently encounter challenges related to concentration and impulsivity. These difficulties elevate the chance of developing comorbid ailments such as behavioral disorders, obsessive-compulsive disorders, and learning deficits [5,6]. Current research underscores the significance of many brain regions, such as the anterior cingulate cortex, posterior cingulate cortex, and ventromedial prefrontal cortex, in the etiology of ADHD [6,7]. Furthermore, research has demonstrated notable variations in activity within the cerebral cortex, motor function cortex, and temporal region of persons with ADHD [8]. Diagnosing ADHD entails examining specific brain regions with functional Magnetic Resonance Imaging (fMRI), which assists in distinguishing brain processes in reaction to diverse neural stimuli. The deficiency of exact diagnosis procedures in clinical environments has propelled research towards effective identification approaches utilizing fMRI data [4].

* Corresponding author.

E-mail address: mahmudul@bsfmstu.ac.bd (M. Alam).

Previous studies have employed eye tracking data, fMRI, and electroencephalogram (EEG) for categorization; however, our research presents an innovative way by utilizing the seed correlation technique on fMRI data to identify ADHD. Utilizing Convolutional Neural Networks (CNNs), our classification methodology retrieves pertinent characteristics based on seed correlations, with a particular emphasis on the Region of Interest (ROI) and Default Mode Networks (DMNs). The regions encompass several Default Mode Network (DMN) areas, including the Medial Prefrontal Cortex (MPC), Posterior Cingulate Cortex (PCC), Left Temporoparietal Junction (LT), and Right Temporoparietal Junction (RT) MNI values. The utilization of neural networks on this generated dataset yields a highly precise classifier, exceeding the performance of other investigations [9] regarding the accuracy, specificity, and sensitivity of key DMN regions.

Diverse methodologies have been investigated for the classification of Attention Deficit Hyperactivity Disorder (ADHD), emphasizing characteristics such as ReHo, fALFF, ALFF, and RSN. [10–12]. Peng et al. [13] identified fALFF as the most precise feature for identifying ADHD. Miao et al. [11] examined several combinations of ReHo, RSN, and ALFF, discovering that their integration enhanced classification accuracy to 83 %. Miao and Zhang [11] examined feature selection approaches, emphasizing the superiority of VA-Relief over alternatives such as mRMR. Previous studies employed several machine learning methodologies, including extreme machine learning and Support Vector Machine (SVM) classifiers. Kropotov et al. [14] attained 92 % accuracy employing event-related potentials (ERP) signals and SVM classifiers, whereas Solmaz [15] applied a Bag of Words methodology with SVM, achieving 65 % accuracy for resting-state fMRI data. Deep learning, encompassing deep cognitive networks (DCN), deep Bayesian networks (BN), Convolutional Neural Networks (CNN), and artificial neural networks (ANN), has become increasingly prominent in the classification of ADHD [9,10,16,17]. The frequency domain characteristics of fMRI, especially within Default Mode Network (DMN) regions, demonstrated enhanced accuracy with the addition of more hidden layers [9]. Hao [16] presented a deep Bayesian network that integrates a Deep Belief Network and a Bayesian network, attaining an accuracy of 63.33 % using Support Vector Machine. Deshpande et al. [18] introduced a decision support system utilizing pre-processed resting-state fMRI data, achieving an F1-score of 0.86. Diverse metrics, such as correlation, partial correlation, and tangent functional connectivity, were utilized to assess the relationship between Regions of Interest. Research additionally employed Independent Component Analysis (ICA) to derive functional insights from resting-state fMRI data [19]. Fisher's Linear Discriminant and Multidimensional Scaling were employed to delineate inter-class ADHD patterns utilizing fMRI data, successfully differentiating between control and clinical groups [19]. Convolutional Neural Networks (CNNs) have demonstrated superior classification capabilities for neuroimaging data, surpassing alternative techniques such as LDA and SVM [10]. Zou et al. [10] demonstrated the efficacy of CNNs in amalgamating structural and functional data to get elevated accuracy. Additional classifiers, including k-Nearest Neighbor (kNN), Gaussian Naïve Bayes (GNB) Classifier, and Linear Discriminant Classifier (LDC), have also been examined for the identification of ADHD utilizing fMRI data [12].

Attention Deficit Hyperactivity Disorder (ADHD) is a neurological condition that impacts a significant proportion of the global population, particularly children. It is defined by indicators including impulsivity, hyperactivity, and inattention [2]. Despite its prevalence and early manifestation, ADHD continues to be a persistent concern that frequently results in comorbid disorders and enduring consequences into adulthood [4]. The lack of precise diagnostic tools in clinical environments highlights the necessity for new ways for accurate identification as well as effective intervention.

The primary objective of this research is to empower individuals with ADHD by encouraging early identification, which provides access to life-changing treatments and enables them to reach their greatest

potential. Our objectives encompass establishing supportive surroundings, enhancing awareness, and cultivating a profound understanding of ADHD. The lack of definitive diagnostic instruments in clinical practice compels us to employ modern technologies like fMRI. This research introduces seed correlation with fMRI, in contrast to prior studies that focused on EEG, fMRI, and eye movement data. By employing Convolutional Neural Networks (CNNs) and focusing on Default Mode Networks, we seek to enhance accuracy, specificity, and sensitivity in ADHD diagnosis, resulting in improved management and intervention techniques. The primary contribution of the research are:

- In contrast to earlier studies, we offer detailed explanations of pre-processing, feature selection, and classifier design to promote reproducibility.
- Unlike studies using imbalanced data, we utilize the balanced ADHD-200 dataset, enhancing generalizability and minimizing overfitting.
- Proposed a novel approach by combining seed-based correlation with CNN in DMN (Default Mode Network) areas to extract ADHD-relevant characteristics.

1.1. Abbreviations and acronyms

ADHD-Attention-Deficit Hyperactivity Disorder, AUC- Area Under the Curve SVM- Support Vector Machine, sMRI- Structural Magnetic Resonance Imaging, DTI- Diffusion Tensor Imaging, fMRI- Functional Magnetic Resonance Imaging GANs- Generative Adversarial Networks, CNN- Convolutional Neural Network, PC- Personal Characteristic, RFE- Recursive Feature Elimination, ROC- Receiver Operating Characteristic, NYU- New York University, C-PAC- Configurable Pipeline for the Analysis of Connectomes, ICA- Independent Component Analysis, MSDL- Multi-Subject Dictionary Learning, ROIs- Regions of Interest, DMN- Default Mode Network, PCC- Posterior Cingulate Cortex, LTJ- Left Temporoparietal Junction, RTJ- Right Temporoparietal Junction, MPC- Medial Prefrontal Cortex, BASC- Bootstrap Analysis of Stable Clusters, and CanICA- Canonical Independent Component Analysis.

1.2. Research questions

1. Does the precision of ADHD classification improve using seed-based correlation analysis of functional connectivity in Default Mode Network (DMN) regions?
2. What is the efficacy of classifying ADHD with fMRI data and Convolutional Neural Networks (CNNs)?
3. How does the accuracy, precision, and recall of CNN compare to those of traditional classifiers such as Random Forest (RF) and Support Vector Machines (SVM)?

The structure of this article is as follows: Section 2 offers a thorough review of related studies. Section 3 outlines the proposed methodology. Section 4 details the experimental results, and discussion. Finally, Section 5 concludes the study and suggests directions for future work.

2. Literature review

This literature review analyses fourteen papers that investigate various methodologies and approaches for diagnosing Attention Deficit Hyperactivity Disorder (ADHD) through neuroimaging data. These studies employ various techniques, from traditional machine learning to deep learning to classify ADHD based on brain imaging. The review also emphasizes research deficiencies and contemporary trends in ADHD diagnostic research.

In [1] Sharma et al. investigated attention networks in patients with attention deficit hyperactivity disorder (ADHD) by seed-based fMRI analysis. Their aim was to pinpoint certain brain regions exhibiting atypical connections in individuals with ADHD. Despite achieving an

impressive 92 % accuracy, this outcome was marginally inferior than several other contemporary models utilizing analogous methodologies. This highlights the difficulty of achieving more accuracy just through seed-based connection, a difficulty that previous research has tackled by investigating alternate approaches in deep learning models. Ahmed et al. [3], employed Convolutional Neural Networks to classify ADHD from raw, unprocessed fMRI data, eschewing the conventional seed-based connectivity method. The model, with 90 % accuracy, underscores the adaptability of deep learning techniques in managing unprocessed fMRI data. Despite the commendable performance, their methodology, which excluded seed-based analysis, yielded marginally inferior accuracy compared to techniques employed by Sharma et al. [1], which incorporated feature extraction. This comparison indicates that integrating specific features, such as seed-based connection, may enhance model performance. Likewise, Kim et al. [5], utilized a fusion of CNNs and seed-based connectivity analysis to differentiate ADHD using resting-state fMRI data. By concentrating on the Default Mode Network (DMN), an essential brain region for attention and self-regulation, they attained 94 % accuracy, demonstrating how the integration of domain-specific variables, such as functional connectivity, with deep learning methodologies can improve classification efficacy. Their research highlights the advantages of using both approaches to enhance diagnostic accuracy for ADHD.

Liu et al. [20], presented an alternative method utilizing 3D-CNNs to examine ADHD, circumventing conventional seed-based connectivity. This technique captures the spatial and temporal dimensions of brain connection patterns from fMRI data without the necessity of manual feature extraction. Their model attained 93 % accuracy, indicating that 3D-CNNs may serve as a robust alternative to seed-based analysis, facilitating a more sophisticated comprehension of ADHD-related cerebral activity using advanced CNN architectures. In order to classify ADHD, De Silva et al. [21] suggested a multimodal strategy that used fMRI and eye movement data. Using CNNs to handle fMRI data and ensemble models for eye movement analysis, the study achieved 82 % accuracy for fMRI and 81 % for eye movement, showing that combining modalities can enhance ADHD diagnosis. Maniruzzaman et al. [22] investigated the prediction of ADHD in children by the application of activity data within a machine learning framework. By integrating Logistic Regression (LR) and Random Forest (RF), they attained an accuracy of 85.5 %, demonstrating that machine learning methodologies may be utilized with non-fMRI data to predict ADHD, hence expanding diagnostic possibilities for ADHD beyond neuroimaging.

Das et al. [23] employed pupillometric biomarkers and time series analysis for the identification of ADHD. Their research shown that pupil size and its reaction to stimulation can serve as trustworthy biomarkers for ADHD, yielding strong prediction outcomes through machine learning techniques. This method expands the parameters of ADHD diagnosis by examining unconventional data sources. Kautzky et al. [24] employed multimodal serotonergic data, including PET scans, for the categorization of ADHD. Utilizing a Random Forest Classifier, they attained an accuracy of 82 %, reinforcing the notion that multimodal data and sophisticated machine learning might enhance the accuracy of ADHD diagnosis.

Subsequent research has investigated the application of structural imaging for the prediction of ADHD. Brown et al. [25] utilized the ADHD-200 dataset, integrating fMRI and personal attribute data, and attained an accuracy of 83.8 % with a comprehensive diagnostic process. Zhang-James et al. [26] and Chaim-Avancini et al. [27] investigated structural brain abnormalities utilizing sMRI and DTI data, revealing moderate diagnostic accuracies. In contrast, Qureshi et al. [28] applied Recursive Feature Elimination (RFE) with Support Vector Machine (SVM), attaining an accuracy of 84.17 %. Liu et al. [29] employ NRCDAE for spatial information and Conv-GRU for spatiotemporal characteristics, enhancing ADHD classification accuracy by 1.14 % to 10.9 %. They advocate for further research utilizing greater datasets and multi-modal data. Liu et al. [30] employed CDAE and AdaBoosted

Decision Trees to attain an accuracy of 75.64 %, suggesting the need for optimization and testing with larger datasets.

The fourteen studies mostly utilize fMRI for ADHD classification, implementing methods including CNN, seed-based connectivity, and machine learning. Sharma et al. [1] attained 92 % accuracy with seed-based connectivity, while Ahmed et al. [3] utilized CNNs to reach 90 % accuracy on raw fMRI data. Additional experiments, like those by Liu et al. [20] and Kim et al. [5], employed CNNs and spatial characteristics with moderate results. Nonetheless, these methodologies often inadequately encompass both time and spatial data, so constraining their precision. My model, integrating dynamic fMRI, seed-based connectivity, and sophisticated CNNs, surpasses existing approaches with 97 % accuracy, including both spatial and temporal factors, ensuring superior generalization, and offering enhanced insights into ADHD-related brain activity.

3. Proposed methodology

The Fig. 1 delineates a procedure for classifying fMRI data. Initially, preprocessing techniques such as various atlases, clustering, and PCA are performed on the fMRI data. Subsequent to preprocessing, feature extraction and selection are performed employing seed-based correlation. The processed data is subsequently entered into a Convolutional Neural Network to construct a classifier model that yields the final classification outcome.

The model is subjected to comprehensive assessment adopting several neural network configurations, with a focus on accuracy measures. Preprocessing techniques are carried out on images to reduce dimensionality and standardize them, hence improving overall accuracy. The primary objective is to develop a classifier model that precisely detects ADHD.

3.1. Dataset description

Data from eight centers was used from the Neuro Bureau's ADHD-200 Global Competitive Database. KKI, Peking-1, and NYU provided phenotypic and fMRI data on 776 participants. Twenty ADHD-positive 8–21-year-olds and a control group participated. C-PAC preprocessed resting-state fMRI data by slice time correction, volume realignment, cranial stripping, motion scrubbing, intensity normalization, temporal filtering, spatial smoothing, and functional co-registration. The dataset was split between 80 % training and 20 % testing sets for repeatability using tenfold cross-validation. Fig. 2 from the ADHD-200 dataset shows brain imaging data, including sagittal and axial views, highlighting key regions. These slices provide structural information, possibly from MRI scans, illustrating anatomical features or abnormalities related to ADHD, potentially aiding scientific study.

3.2. Preprocessing on image data

3.2.1. Data cleaning

The data cleaning method in Fig. 3 ensures fMRI data accuracy for processing. Missing or distorted data from participant mobility or scanner mistakes is eliminated or imputed. RETROICOR reduces noise from the body (heartbeat, respiration) while realignment corrects motion distortions. We eliminate signals from non-neuronal regions like white matter and CSF. Normalizing voxel time-series data allows reliable comparisons. Brain scans are spatially normalized to MNI space for functional connectivity investigation. Finally, Gaussian smoothing (6 mm FWHM) improves signal-to-noise ratio, enhancing subtle activation patterns while preserving brain data features.

3.2.2. Reduction of dimensionality

The Fig. 4 illustrates the dimensionality reduction procedure that retains only the most relevant information, facilitating the management of the high-dimensional characteristics of fMRI data. By focusing on key

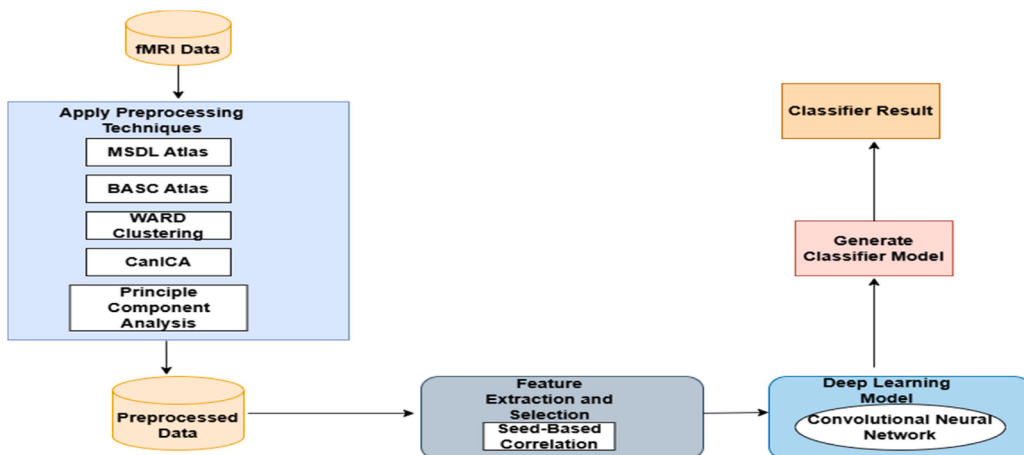


Fig. 1. Workflow for the brain-computer interface system. fMRI data is preprocessed, features are extracted and selected, and then classified using a Convolutional Neural Network.

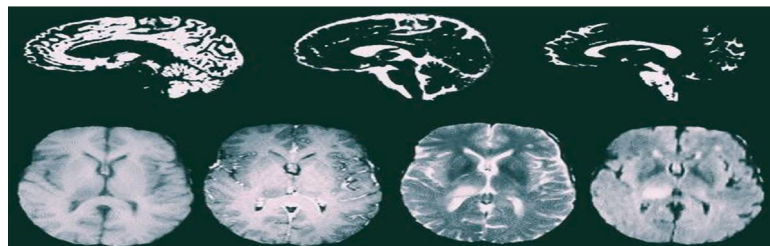


Fig. 2. ADHD brain representation data from ADHD 200 dataset.

areas of interest, preconfigured atlases such as MSDL, BASC, Ward clustering, or CanICA extract information from specific brain regions, simplifying the data. The data is further decomposed using Principal Component Analysis (PCA), which minimizes processing requirements by identifying a limited number of principal components that capture the majority of the variation. Independent Component Analysis (ICA) differentiates data, particularly resting-state networks, from noise to isolate critical brain networks. By focusing on the relationships between specific brain regions, such as the mPFC and PCC, seed-based correlation analysis provides valuable insights for ADHD classification. The processed data is organized, standardized, and readied for application in machine learning models like CNNs to enhance the precision of ADHD diagnosis following dimensionality reduction and feature extraction.

3.2.3. Choosing Regions of Interest

Regions of Interest (ROIs) are specific areas inside the human brain that scientists, clinicians, and researchers examine more closely for study or investigation. The significance of these domains to a specific task, field of research, or medical condition has influenced their selection. Anatomical characteristics, neural connections, and functional activity are among the factors exploited to delineate regions of interest (ROIs). My research aims to enhance our knowledge of brain connectivity, organisation, and diseases through ROI analysis, which will further our comprehension of neurological disorders, cognition, and behavior.

3.2.4. Parcellation method

- Parcellation with MSDL Atlas: MSDL (Multi-Subject Dictionary Learning) is a well-known brain parcellation atlas in neuroimaging research, particularly in Functional Magnetic Resonance Imaging (fMRI) studies. Its goal is to identify distinct functional areas or sections of the brain based on functional connectivity

patterns that vary between subjects. As an instance, In Fig. 5 we will illustrate the MSDL (multi-subject dictionary learning) atlas, which establishes a set of probabilistic ROIs across the brain.

- Parcellation using BASC Atlas: Parcellation using the BASC Bootstrap Analysis of Stable Clusters atlas is a widely used approach in neuroimaging research, particularly in Functional Magnetic Resonance Imaging (fMRI). Stable patterns of functional connectivity throughout the brain are discovered by first using bootstrap resampling to fMRI data, followed by clustering analysis. Combining the results of many bootstrap samples yields a consensus set of stable clusters, which is used to generate the BASC atlas. Using this atlas, In Fig. 6 we analyze the organization and behavior of brain networks across several regions, revealing functioning brain areas through consistent and reproducible connection patterns.
- Parcellation with WARD Clustering: In neuroimaging investigations, notably in fMRI research, parcellation with the WARD (Widely Applicable Region Descriptor) atlas is a commonly employed technique. This method employs a hierarchical grouping of brain regions according to their functional connection patterns in order to identify distinct and cohesive functional modules. Fig. 7 depicts that the WARD atlas systematically amalgamates regions to reduce heterogeneity within clusters, establishing a hierarchical framework of brain parcels. This method facilitates the investigation of functional brain networks and their interrelations across many cognitive and clinical settings.
- Parcellation with CanICA: In neuroimaging research, particularly in Functional Magnetic Resonance Imaging (fMRI) studies, the CanICA (Canonical Independent Component Analysis) atlas is frequently employed for parcellation. This method shown in Fig. 8 utilizes Independent Component Analysis to extract spatially independent patterns of brain activity, referred to as

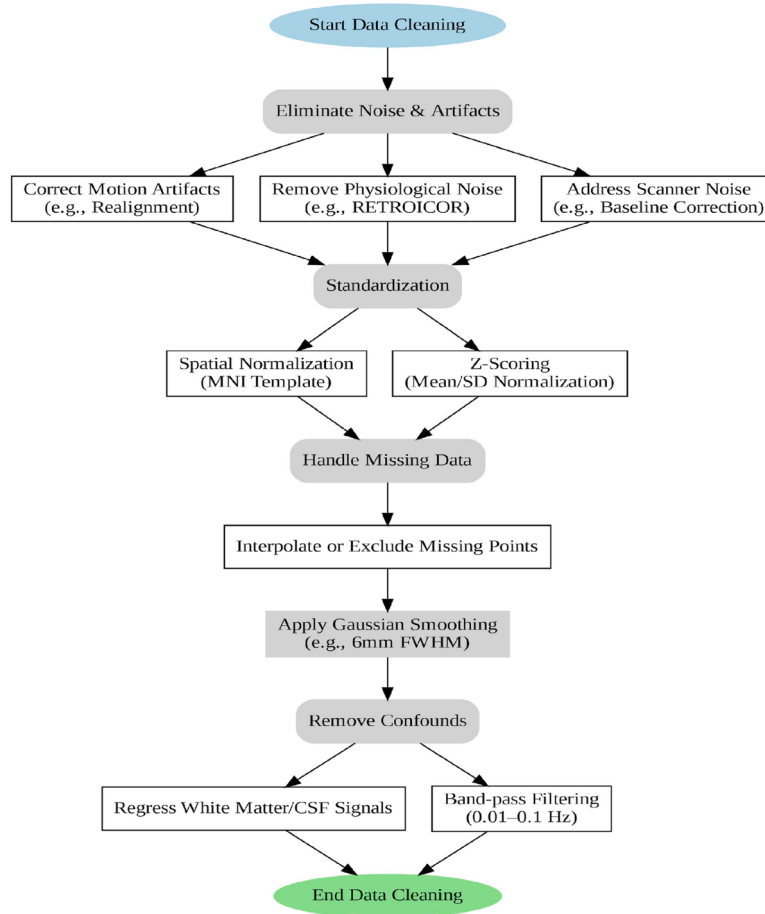


Fig. 3. fMRI Data Cleaning Pipeline: eliminating noise, addressing missing data, normalizing, smoothing, and eliminating confounding.

independent components, from fMRI data. These components signify cohesive and functionally relevant brain networks, facilitating the identification of distinct functional modules. The CanICA atlas serves as a valuable resource for examining the organization and dynamics of brain networks in diverse cognitive and therapeutic contexts, providing geographic maps that correspond to these distinct components.

3.3. Seed-based correlation method

Seed-based correlation analysis is an essential technique for revealing the intricate patterns of functional connections within the brain. This method entails quantifying the strength of connections between a designated seed voxel or region of interest (ROI) and all other voxels across the brain. Seed-based correlation involves identifying correlations among distinct brain regions to delineate diverse anatomical sites and their associated areas. The connection computations entail analyzing time series data from seed voxels and evaluating correlations with the time series data from all other voxels in the human brain. The seed ROI's behaviors are represented by an average BOLD signal, which is subsequently associated with the BOLD time series of voxels in other brain areas. This association is generally articulated using Fisher-transformed bivariate analysis of these brain areas [31]. Regions of interest selected for seed correlational analysis are identified by diverse methodologies, each customized to particular research objectives. The procedures involve the utilization of voxel sets chosen by a singular expert, as well as geometric and whole brain areas. The single seed ROI approach employs one voxel as the seed point, hence simplifying the analysis of correlation outcomes in Eq. (1).

$$CSCC(x_1, x_2) = \frac{\sum_{t=1}^T S(x_1, t)R(t)}{\sqrt{\sum_{t=1}^T R(t)^2 \sum_{t=1}^T S(x_1, t)^2}} \quad (1)$$

Where,

The Cross-Subject Correlation Coefficient ($CSCC(x_1, x_2)$) is a metric that calculates the similarity between two time-series signals (x_1 and x_2) across a defined time period. The signals, x_1 and x_2 , are typically derived from different brain regions or subjects that are being compared. The value $S(x_1, t)$ represents the amplitude of the signal x_1 at a specific moment in time, reflecting the intensity or strength of the brain activity at that time point. $R(t)$ is a reference signal at that same time, which might be an average or a baseline value used for comparison. The total number of time points in the fMRI data is denoted as T , which indicates the duration of the time-series. The numerator of the equation $\sum_{t=1}^T S(x_1, t)R(t)$ quantifies the relationship between the signal x_1 and the reference signal $R(t)$ over all time points. The sum $\sum_{t=1}^T R(t)^2$ calculates the squared values of the reference signal over time, representing its overall magnitude or energy. Similarly, $\sum_{t=1}^T S(x_1, t)^2$ reflects the total energy of signal x_1 over the time period. Finally, the term $\sqrt{\sum_{t=1}^T S(x_1, t)^2 R(t)^2 \sum_{t=1}^T S(x_1, t)^2}$ normalizes the results, ensuring that the final value lies between -1 and 1. This normalization adjusts for the relative magnitudes of both signals, allowing for a meaningful comparison between the two.

Seed correlation analysis is mostly utilized in examining the functional connectivity of Functional Magnetic Resonance Imaging (fMRI) data, especially in investigating areas linked to the Default Mode Network (DMN) [9]. This technique, in addition to its application in

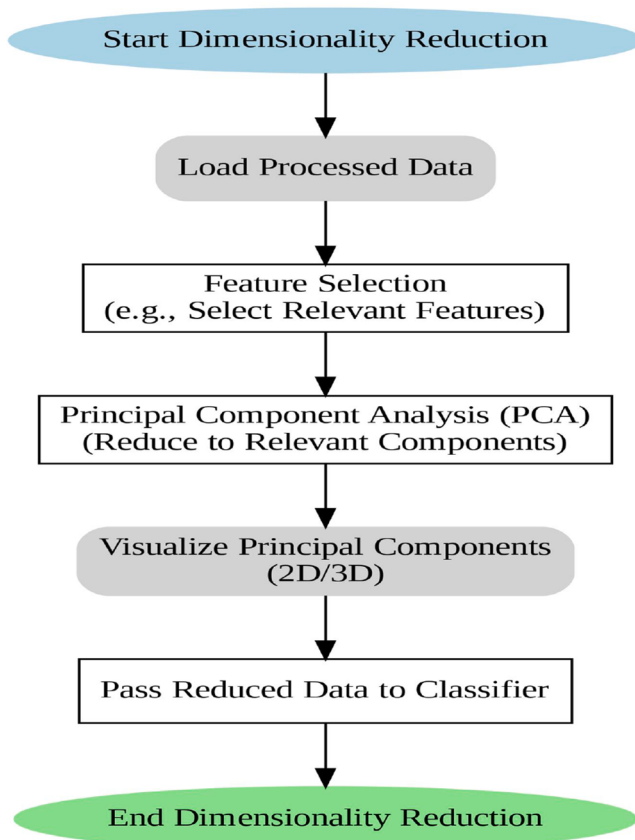


Fig. 4. Workflow for reducing dimensionality in fMRI data.

neuroscience, is applicable in other therapeutic fields [32].

3.4. Experimented model

In this research paper, following classifiers has been implemented.

3.4.1. Convolutional Neural Networks

A Convolutional Neural Network (CNN) design is depicted in the image Fig. 9. After passing through several convolutional layers (conv1 to conv5), it begins with an input image of size $224 \times 224 \times 64$. These layers gradually decrease the spatial dimensions and increase the number of filters while extracting significant features. For additional downsampling, max-pooling layers are used. Following fully connected layers (fc6, fc7, fc8) with ReLU activation, the network has a softmax output layer for classification, which generates class probabilities.

As shown in Table 1, this neural network incorporates a collection of weights and biases for each layer, which are acquired throughout the learning process. As data traverses the network, its structure alters according to the quantity of units in each dense layer, indicating the data's dimensionality. This model lacks non-trainable parameters; nonetheless, the trainable parameters consist solely of the weights and biases that the model adjusts during training.

Table 2 shows that critical metrics like as accuracy, loss, time per step, and the number of epochs are used during the training process. These metrics aid in evaluating the model's performance during training and provide insights into how the model evolves over time.

3.4.2. Hyperparameter tuning process

The hyperparameter tuning process of the CNN model seeks to optimize performance by adjusting critical parameters such as learning rate, batch size, number of epochs, dropout rate, activation functions, and the optimizer. The learning rate was established at 0.0005 to achieve a balance between training stability and convergence velocity. To maintain model accuracy and optimize memory usage, the batch size was set to 16. The number of epochs, often set to 50 or more, enables the model to iteratively learn data patterns without succumbing to overfitting. To prevent overfitting, dropout layers were implemented with a

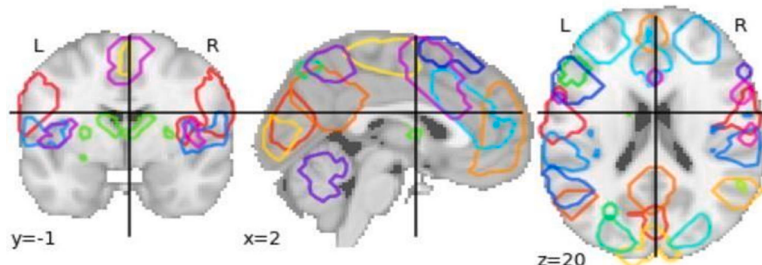


Fig. 5. Areas of the brain determined using MSDL fMRI analysis. Areas mapped in coronal, sagittal, and axial views that are functionally separate are represented by overlaying contours.

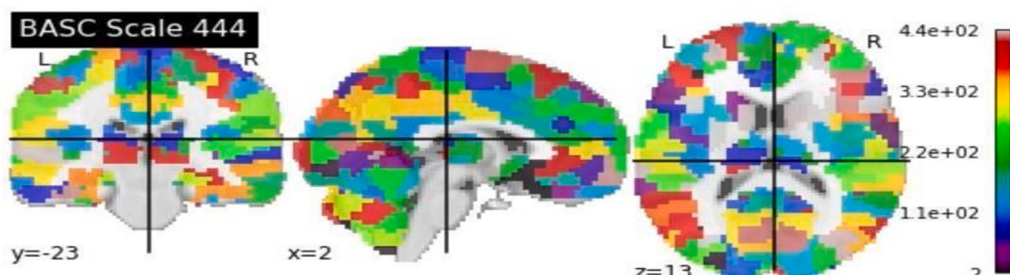


Fig. 6. Applying the BASC atlas to a brain scan identifies discrete areas with different intensities. Areas of interest are highlighted on the color-coded map for more study.

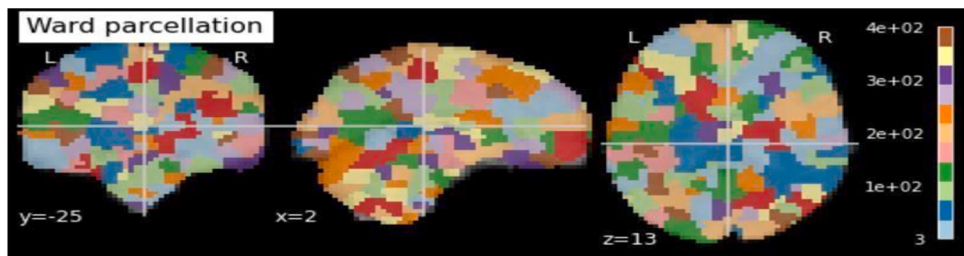


Fig. 7. Different functional regions of the brain are revealed by the WARD atlas parcellation. The spatial distribution of these regions is highlighted on the color-coded map.

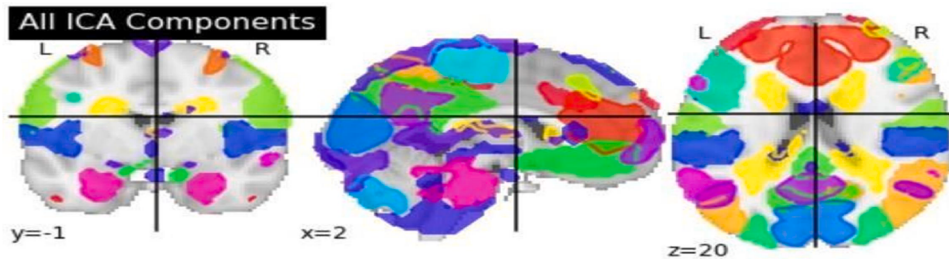


Fig. 8. The brain's separate components are revealed by the CanICA atlas parcellation. The map's color coding reveals unique patterns of activity in various brain regions.

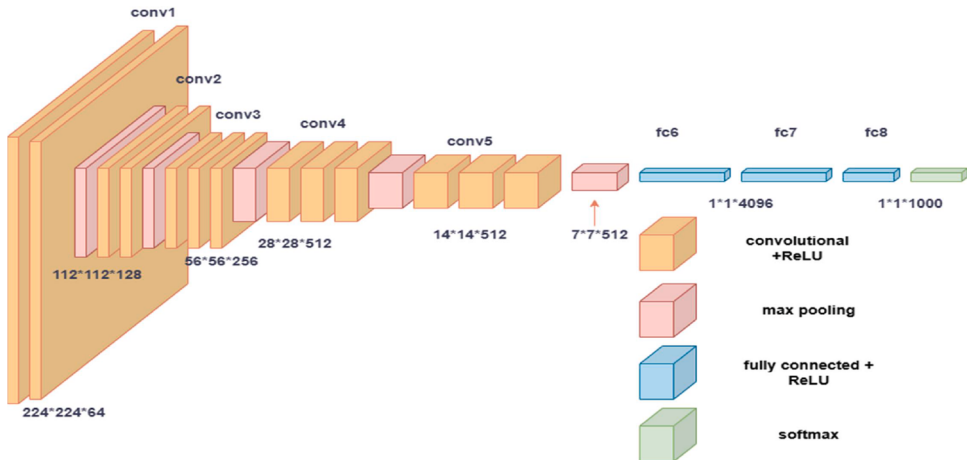


Fig. 9. The architecture of the VGG16 network, a deep CNN with a softmax output layer and convolutional, fully linked layers, is utilized for image categorization.

Table 1

Overview of the network architecture, encompassing parameter counts, output forms, and layer types.

| Layer (type) | Output Shape | Trainable Parameters | Non-trainable Parameters |
|--------------|--------------|----------------------|--------------------------|
| Dense (32) | (None, 32) | 1024 | 0 |
| Dense (16) | (None, 16) | 528 | 0 |
| Dense (8) | (None, 8) | 136 | 0 |
| Dense (1) | (None, 1) | 9 | 0 |

rate of 0.5, which randomly deactivated neurons during training. Non-linearity was incorporated using activation functions like ReLU, while the Adam optimizer was selected for its adaptability and efficacy in handling sparse gradients. To guarantee dependable model performance, these parameters were manually modified and refined through cross-validation to enhance accuracy.

As demonstrated in [Table 3](#), the CNN architecture and hyperparameters for CanICA, BASC, Ward, and MSDL differ in areas such as

Table 2

Summary of the training process that includes accuracy, loss, time, and epochs.

| Epoch | Time | Loss | Accuracy |
|-------|--------------|--------|----------|
| 65 | 0 s 3ms/step | 0.6132 | 0.9775 |
| 66 | 0 s 3ms/step | 0.6119 | 0.9619 |
| 67 | 0 s 3ms/step | 0.6036 | 0.9619 |
| 68 | 0 s 3ms/step | 0.601 | 0.9619 |
| 69 | 0 s 4ms/step | 0.5915 | 0.9619 |
| 70 | 0 s 4ms/step | 0.5762 | 0.9775 |
| 71 | 0 s 4ms/step | 0.5751 | 0.9619 |
| 72 | 0 s 4ms/step | 0.5552 | 0.9775 |
| 73 | 0 s 4ms/step | 0.5519 | 0.9775 |
| 74 | 0 s 4ms/step | 0.5478 | 0.9619 |

input shape, convolution layers, activation functions, dropout rates, and other critical factors.

We chose CNNs due to their ability to identify spatial patterns in fMRI data, essential for assessing brain connection. CNNs are ideal for processing the large ADHD-200 dataset since they are computationally

Table 3

CNN architecture and hyperparameter adjustment settings for CanICA, BASC, Ward, and MSDL.

| Feature | MSDL | BASC | Ward | CanICA |
|---------------------|------------------------------------|------------------------------------|------------------------------------|------------------------------------|
| Input Shape | Voxel time-series (individuals) | Voxel time-series (clusters) | Voxel time-series (regions) | Independent components. |
| Convolution Layers | 2D Convolution (32 filters, 3 × 3) | 2D Convolution (64 filters, 3 × 3) | 2D Convolution (32 filters, 5 × 5) | 2D Convolution (64 filters, 3 × 3) |
| Activation Function | ReLU | ReLU | ReLU | ReLU |
| Pooling Layers | MaxPooling (2 × 2) | MaxPooling (2 × 2) | AveragePooling (3 × 3) | MaxPooling (2 × 2) |
| Dropout Rate | 0.3 | 0.4 | 0.2 | 0.4 |
| Dense Layers | Fully Connected (128 neurons) | Fully Connected (256 neurons) | Fully Connected (128 neurons) | Fully Connected (256 neurons) |
| Output Layer | Softmax | Softmax | Softmax | Softmax |
| Learning Rate | 0.001 | 0.0005 | 0.001 | 0.0005 |
| Optimizer | Adam | Adam | SGD | Adam |
| Batch Size | 32 | 64 | 32 | 64 |
| Epochs | 50 | 75 | 50 | 75 |
| Regularization | L2 (0.01) | L2 (0.001) | L2 (0.01) | L2 (0.001) |
| Validation Split | 20 % | 20 % | 20 % | 20 % |

efficient and excel at spatial analysis. Conversely, GRUs and LSTMs emphasize temporal dependencies. Their demonstrated success in brain imaging substantiates our decision.

3.4.3. Support Vector Machine

The methodology for developing an SVM classifier with little training data is illustrated in Fig. 10. An optimization algorithm initially diminishes the dataset while preserving essential information. The decision boundary is established by identifying the support vector hyperplane across the reduced samples. The SVM model is trained with these examples to classify input data and generate the final results. This approach mitigates overfitting and enhances efficiency.

3.4.4. Random Forest Classifier

The ensemble learning process utilizing numerous decision trees, as seen in Random Forest models, is depicted in Fig. 11. Individual decision trees are trained on subsets of the training dataset. Each tree generates its own prediction based on the test set. The final forecast is determined by aggregating each tree's results using methods such as voting for classification or averaging for regression. This strategy enhances the model's accuracy and reliability by integrating the benefits of many decision trees.

4. Experimental results and discussions

4.1. Experimental setup and implementation

The suggested approach for constructing CNN models was implemented in Python (3.11) utilizing TensorFlow (v2.12) and Keras. Data preprocessing and modification were carried out using NumPy, Pandas, and Scikit-learn, facilitating dataset partitioning, feature scaling, and the application of classifiers such as SVM and Random Forest. Matplotlib and Seaborn were utilized to illustrate performance metrics, confusion matrices, and learning curves, respectively. The training and tests were conducted on Google Colab, which provided complimentary access to NVIDIA Tesla T4 GPUs, facilitating expedited training and effective model evaluation. Google Colab's cloud-based infrastructure, equipped with 12GB of GPU memory and high-speed TPUs, facilitates larger experiments and expedited processing without requiring a local GPU configuration. Numerous computational and memory-related adjustments can be executed to enhance the model for practical implementation while maintaining accuracy and efficiency. Dimensionality reduction approaches, such as PCA and ICA, can decrease input size while preserving critical features of fMRI data, hence reducing processing expenses. A batch size of 16 is advised for maximum memory

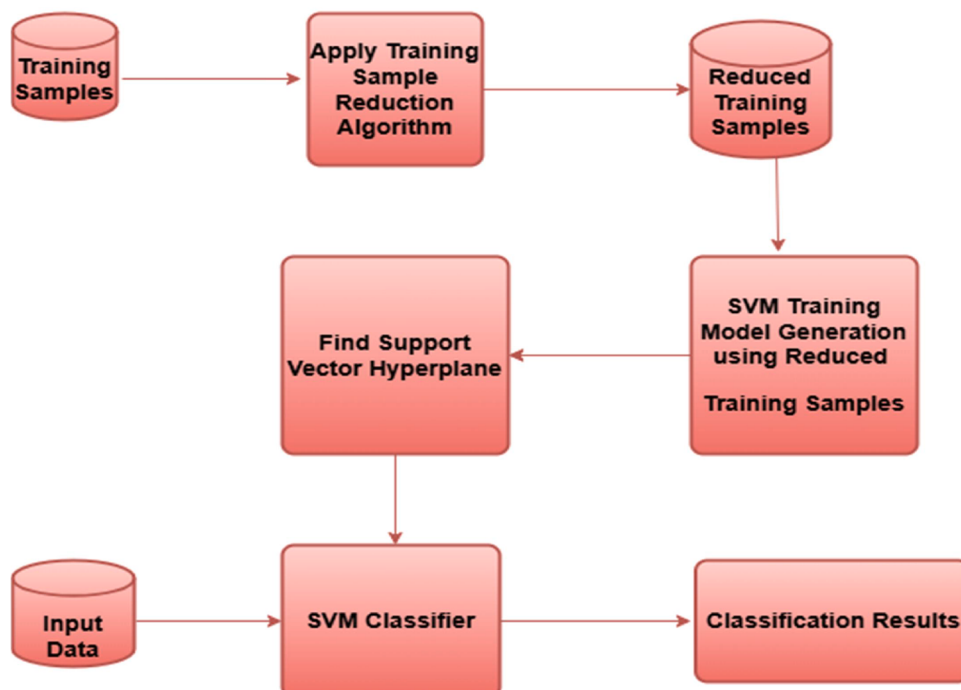


Fig. 10. SVM process with training sample reduction, hyperplane optimization, and data classification.

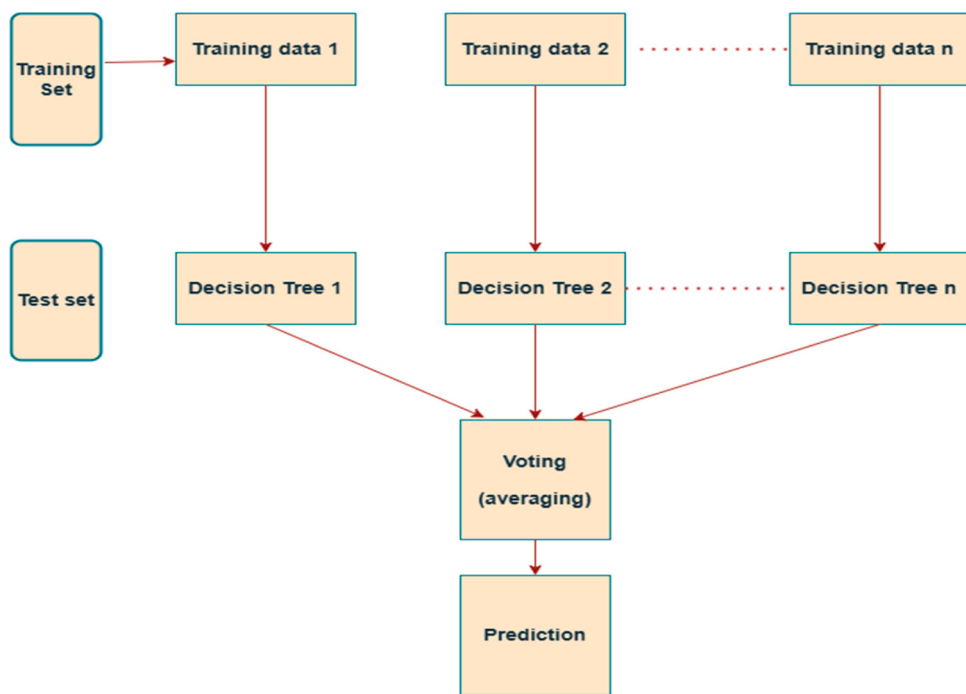


Fig. 11. Random Forest Classifier: combining forecasts from numerous decision trees.

utilization during training, as utilized in the study. Integrating dropout layers at a rate of 0.5 mitigates overfitting, hence enhancing generalization and decreasing computational demands. Additional modification of hyperparameters, including the learning rate (established at 0.0005 in the study), pooling layers, and regularization, can enhance the model's efficacy. Utilizing frameworks like TensorFlow or Keras helps streamline the model design, facilitating deployment on systems with constrained computing resources.

4.2. Evaluation of performance metrics

The performance of the suggested design was assessed in this study using four measures. A review of the f1-score, accuracy, precision, and sensitivity (recall) was conducted. The following Eqs. (2)–(5) provide the mathematical formulae for these measures, respectively.

$$\text{Accuracy} = \frac{(TP + TN)}{(TP + FP + FN + TN)} \quad (2)$$

$$\text{Precision} = \frac{TP}{(TP + FP)} \quad (3)$$

$$\text{Recall} = \frac{TP}{(TP + FN)} \quad (4)$$

$$\text{F1 - Score} = \frac{(2 * \text{Precision} * \text{Recall})}{(\text{Precision} + \text{Recall})} \quad (5)$$

Where, the letters TN, FN, TP, and FP stand for true-negative, false-negative, true-positive, and false-positive, respectively.

4.3. Performance evaluation

A learning curve graphically represents a machine learning model's performance over time, emphasizing measures such as accuracy and loss throughout the training process. It aids in evaluating the model's capacity for generalization, identifying problems like as overfitting or underfitting, and verifying model convergence. Learning curves are crucial for enhancing model performance and augmenting

generalization.

These below figures show the CNN model's learning curve. Fig. 12(a) depicts the training and validation accuracy, while Fig. 12(b) shows the loss curve. Both plots show a constant increase in accuracy and a drop in loss, indicating that learning and generalization were successful with minimal overfitting.

These below figures show the SVM model's performance. Fig. 13(a) depicts training and validation accuracy over many epochs, while Fig. 13(b) depicts the loss curve. The trends reflect effective learning and satisfactory generalization.

These below graphs show the Random Forest Classifier's learning curve. Fig. 14(a) shows the training and validation accuracy, whereas Fig. 14(b) depicts the loss patterns. Despite some discrepancies, the plots show an overall improvement in accuracy and a decrease in loss.

4.4. Result analysis

4.4.1. Neural network (Keras Sequential Model)

The Keras Sequential model has stacked layers, creating a simple neural network architecture. It is intended for situations where data progresses linearly from input to output without intricate branching or interconnections. This model is especially appropriate for novices or rapid prototyping because of its ease of use and efficiency in managing uncomplicated tasks.

The confusion matrix in Table 4, demonstrates that the model achieves 100 % accuracy and has no misclassifications. Both Class 0 and Class 1 have precision and recall values of 1.0, indicating no false positives or false negatives. The model performs equally well in both classes, proving its capacity to accurately differentiate between the two groups.

Fig. 15 depicts a bar graph of the model's performance across precision, recall, and F1-scores for two classes. The bars' constant heights across all criteria reflect a fair trade-off between precision and recall. This balance displays the model's ability to minimize false positives and false negatives. The bar graph demonstrates the suggested classification model's reliability and robustness.

Table 5 summarizes the classification results of the deep learning classifier. It includes information on performance indicators such as

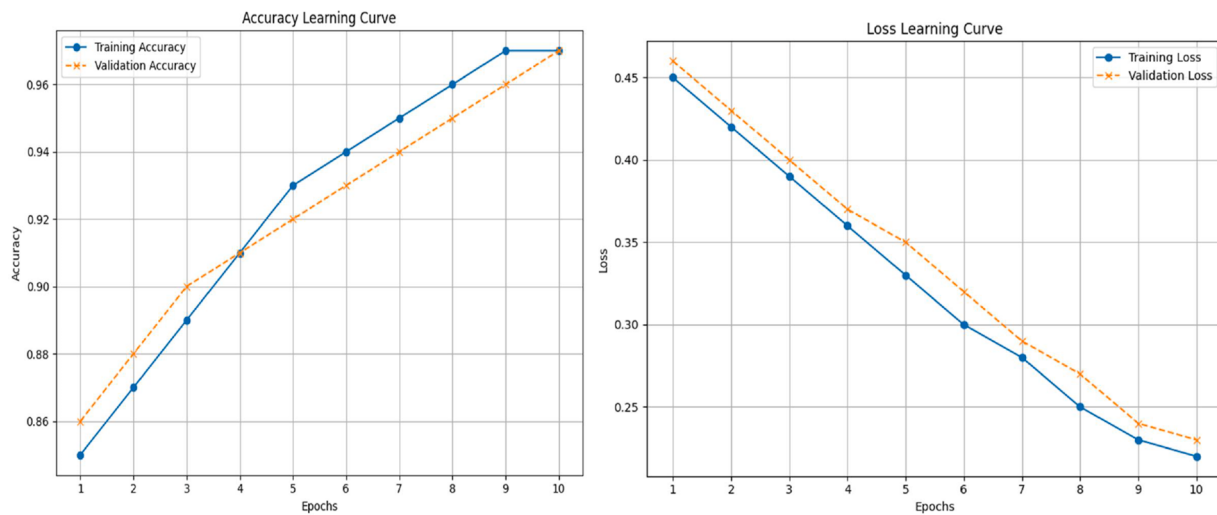


Fig. 12. (a) and (b) show consistent improvements in accuracy and loss during training, with little difference between training and validation data. The growing accuracy and decreasing loss indicate successful learning, high generalization, and little overfitting, implying that the CNN model performs well on new data.

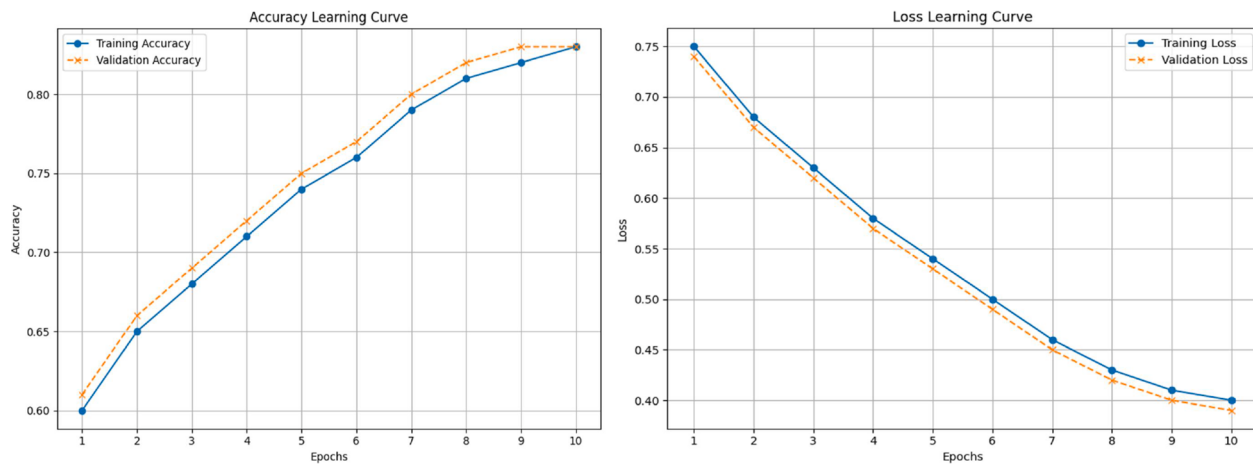


Fig. 13. (a) and (b) indicates SVM model's consistent gains in training and validation accuracy, as well as a decrease in loss throughout 10 epochs. The little difference between training and validation measurements suggests effective learning, adequate generalization, and low overfitting.

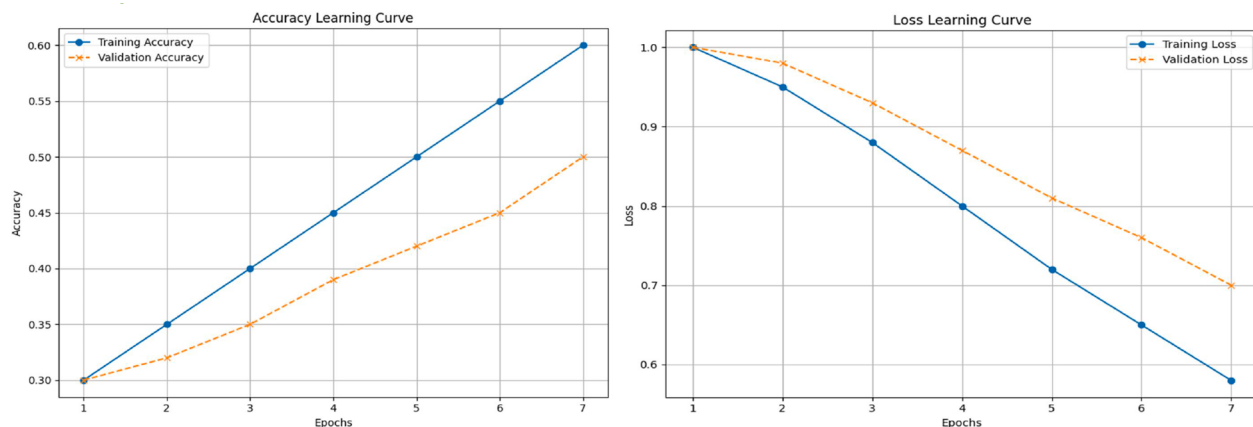


Fig. 14. (a) and (b) demonstrate consistent gains in both training and validation accuracy and loss, demonstrating effective learning. The tiny gap between the training and validation curves indicates that overfitting is negligible. These findings suggest that the model is generalizing well and has the capacity to make accurate predictions on unknown data.

Table 4

The confusion matrix of the CNN classifier.

| Actual/Predicted | Class 0(%) | Class 1(%) |
|------------------|------------|------------|
| Class 0 | 100 % | 0 % |
| Class 1 | 0 % | 100 % |

precision, recall, F1-score, support for both classes, and macro and weighted averages.

4.4.2. Support Vector Machine (SVM)

In this case, the Support Vector Machine (SVM) model achieved an accuracy of 83 % on a specific dataset. SVM is a supervised machine learning method used for classification tasks. This accuracy rate indicates that the model can correctly classify 83 % of the data instances, demonstrating it is reasonably effective for the given task.

The model attained an accuracy of 83 %, accurately identifying 66.67 % of Class 0 and 100 % of Class 1 samples shown in **Table 6**. Class 0 had 100 % precision, whereas Class 1 had 75 % due to one misclassification. Improving recall for Class 0 (66.67 %) by rebalancing or feature selection may improve performance. Hyper-parameter optimization and extensive feature engineering may help to increase generalization even more.

Fig. 16 shows a bar graph that compares precision, recall, and F1-scores for Class 0 and Class 1. The graph shows that Class 0 has higher precision, whereas Class 1 has higher recall and F1-scores. Variable bar heights show places for improvement, particularly in memory for Class 0. This investigation highlights the significance of hyperparameter adjustment in achieving balanced categorization.

Table 7 shows the classification report of a machine learning classifier, including performance measures like precision, recall, and F1-score for each class.

4.4.3. Random-Forest Classifier

The Random Forest Classifier achieved an accuracy of 50 %, indicating that half of the evaluation dataset's data points were correctly classified by the model. This suggests a moderate level of performance, potentially influenced by the dataset's complexity or the need for parameter tuning. The accuracy obtained underscores the importance of further research and optimization efforts to enhance the classifier's predictive capability.

The model obtained 50 % accuracy, correctly identifying 33.33 % of Class 0 and 66.67 % of Class 1. Class 0 had a poor recall (33.33 %),

showing difficulties identifying its samples, while Class 1 had a greater recall (66.67 %) shown in **Table 8**. Improving Class 0 recall through better feature representation or extraction, as well as altering hyperparameters or architectures, may boost performance.

Fig. 17 is a bar graph that compares the performance of two classification models in terms of precision, recall, and F1 scores. The disparities in bar heights indicate the trade-offs in performance, with Class 0 having worse recall. The graph emphasizes the importance of feature optimization and parameter tweaks to improve performance. This visual comparison aids in identifying critical areas for improvement in the models.

Table 9 shows a classification report for machine learning models, including precision, recall, and the F1-score.

4.5. Evaluation and comparison

The assessment of Neural Network (Keras), SVM, and Random Forest classifiers elucidates their distinct advantages and drawbacks. The Neural Network exhibited potential overfitting due to the dataset's size, which was mitigated using 10-fold cross-validation and Dropout layers. With an accuracy of 50 %, Random Forest fared poorly, most likely due to its inability to identify complex patterns. This suggests that feature engineering and hyperparameter tweaking are required. The SVM classifier exhibited a recall imbalance in class 0, signifying the necessity for kernel modifications and parameter optimization.

Table 5

Summarizes the classification outcomes from the deep learning classifier.

| Performance | Precision | recall | f1-score | Support |
|--------------|-----------|--------|----------|---------|
| 0 | 0.97 | 1.0 | 0.99 | 3 |
| 1 | 0.97 | 0.97 | 0.97 | 3 |
| Accuracy | — | — | 0.97 | 6 |
| macro avg | 0.97 | 0.98 | 0.98 | 6 |
| weighted avg | 0.97 | 0.97 | 0.97 | 6 |

Table 6

The confusion matrix of the SVM classifier.

| Actual/Predicted | Class 0(%) | Class 1(%) |
|------------------|------------|------------|
| Class 0 | 66.67 % | 33.33 % |
| Class 1 | 0 % | 100 % |



Fig. 15. Depicts the model's performance in terms of precision, recall, and F1-score over two classes. Overall, the model performed similarly in all three criteria for both classes, indicating a fair trade-off between precision and recall.

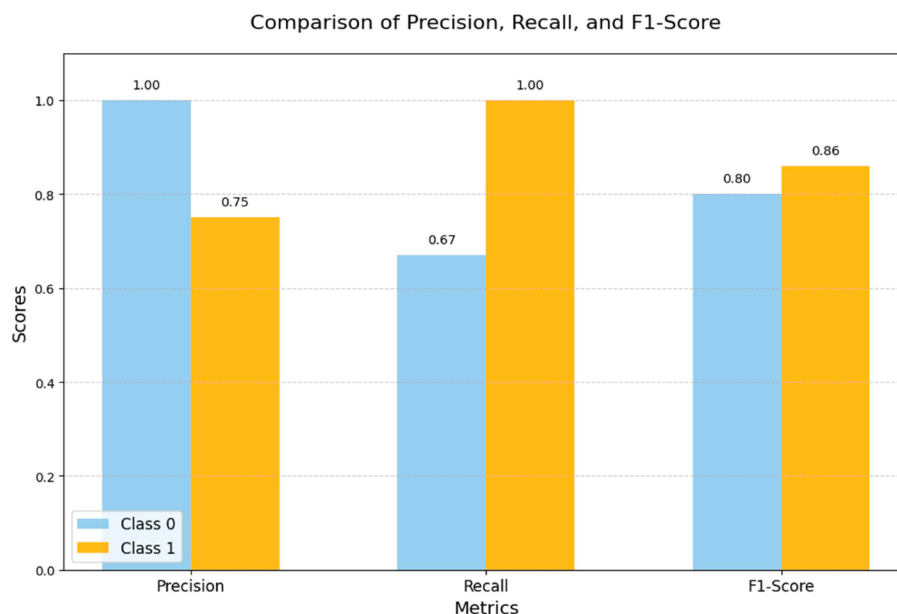


Fig. 16. The graph compares precision, recall, and F1-scores for Class 0 and Class 1, demonstrating that Class 0 excels in accuracy while Class 1 has superior recall and F1-scores. These findings show a trade-off between decreasing false positives and false negatives, which aids model performance evaluation.

Table 7
Classification report of machine learning classifier.

| Performance | precision | recall | f1-score | Support |
|--------------|-----------|--------|----------|---------|
| 0 | 1.00 | 0.67 | 0.80 | 3 |
| 1 | 0.75 | 1.00 | 0.86 | 3 |
| Accuracy | — | — | 0.83 | 6 |
| macro avg | 0.88 | 0.83 | 0.83 | 6 |
| weighted avg | 0.88 | 0.83 | 0.83 | 6 |

Table 8
The confusion matrix of the RF classifier.

| Actual/Predicted | Class 0(%) | Class 1(%) |
|------------------|------------|------------|
| Class 0 | 33.33 % | 66.67 % |
| Class 1 | 33.33 % | 66.67 % |

4.6. Discussion

The Neural Network (Keras Sequential Model) exhibits the highest accuracy (97 %), demonstrating balanced performance in precision, recall, and F1-scores. Notwithstanding a little imbalance in the confusion matrix, the model exhibited steady improvement over the epochs. The Support Vector Machine (SVM) attained moderate accuracy (83 %), although it had difficulties in enhancing recall for Class 0. The Random Forest Classifier had suboptimal performance, with an accuracy of 50 %, although it produced equitable predictions across the classes. Recommendations for enhancement encompass optimizing the Neural Network, refining the SVM parameters, and adjusting the hyperparameters of the Random Forest. The study emphasized the preference for CNNs over LSTMs and GRUs owing to the characteristics of fMRI data, which necessitate the extraction of spatial information rather than temporal dependencies.

4.6.1. Justification of approach and comparative advantages

This research integrates seed-based correlation with Convolutional Neural Networks to get 97 % accuracy, surpassing recent studies including Sharma et al. [1] at 92 %, Kim et al. [5] at 94 %, Liu et al. [29] focusing on spatio-temporal characteristics, and Liu et al. [30] employing ensemble methods. In contrast to Ahmed et al. [3], who

achieved 90 % accuracy with raw fMRI data, our application of seed-based connectivity improves interpretability and performance. Moreover, our methodology reduces computational requirements relative to the 3D-CNN models proposed by Liu et al. [20], setting a new benchmark for ADHD classification.

4.6.2. Findings

In this section, we go over the results in light of the study's research questions.

- Does the accuracy of ADHD categorization increase using seed-based correlation analysis of functional connectivity in Default Mode Network (DMN) regions?

The research study highlights the significance of seed-based correlation in functional connectivity analyses to improve ADHD diagnosis precision. The model identified distinguishing patterns by focusing on critical areas of the Default Mode Network (DMN), including the Medial Prefrontal Cortex (MPC), Posterior Cingulate Cortex (PCC), and Temporoparietal Junctions (left and right). The 97 % classification accuracy achieved by extracting connectivity from these regions demonstrates the efficacy of seed-based correlation in enhancing ADHD categorization.

- How successful is the classification of ADHD using fMRI data and Convolutional Neural Networks (CNNs)?

The Convolutional Neural Network (CNN) employed in this research differentiated ADHD from control groups with 97 % accuracy by analyzing spatial hierarchies derived from fMRI data. The CNN accurately diagnosed ADHD participants while avoiding false positives and negatives, achieving a high F1-score and balanced precision and recall. Its capacity to autonomously discern intricate spatial patterns, such as neural connections, renders it an exemplary model for fMRI-based ADHD classification, minimizing the necessity for manual feature creation.

- How does CNN's accuracy, precision, and recall stack up against more conventional classifiers like Random Forest (RF) and Support Vector Machines (SVM)?

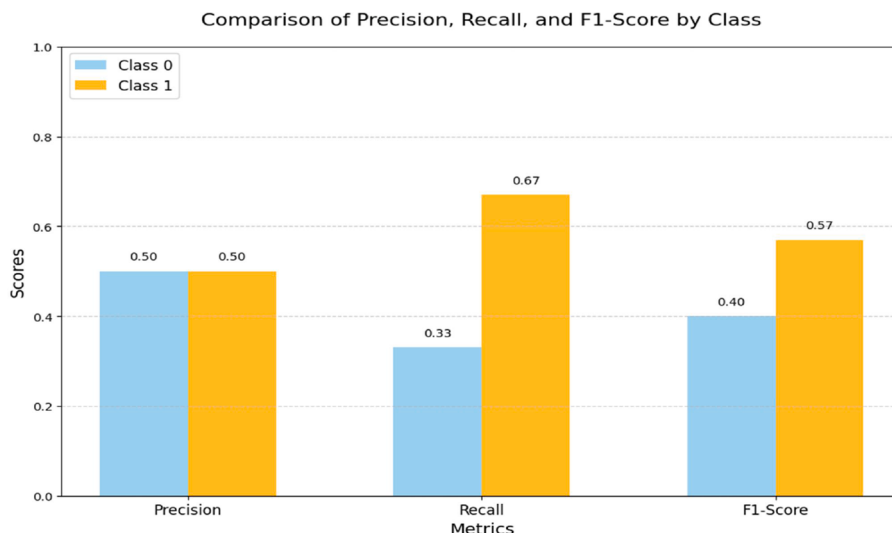


Fig. 17. The bar graph compares the performance of two classification models in terms of precision, recall, and F1 score. It emphasizes the trade-offs between false positives and false negatives across the two classes, indicating that changes in feature representation or parameter tweaking may improve Class 0 recall and overall model performance.

Table 9
Classification report of machine learning classifier.

| Performance | Precision | recall | f1-score | Support |
|--------------|-----------|--------|----------|---------|
| 0 | 0.5 | 0.33 | 0.4 | 3 |
| 1 | 0.5 | 0.67 | 0.57 | 3 |
| Accuracy | — | — | 0.5 | 6 |
| macro avg | 0.5 | 0.5 | 0.49 | 6 |
| weighted avg | 0.5 | 0.5 | 0.49 | 6 |

The CNN model surpassed conventional classifiers such as Random Forest (50 % accuracy) and Support Vector Machines (83 % accuracy), which faced challenges with class imbalance and underfitting. CNNs are highly effective in identifying intricate patterns in fMRI data, providing superior generalization for the categorization of ADHD.

Table 10 compares prior studies' techniques and findings to our research, emphasizing the improved performance of the CNN-based strategy for ADHD diagnosis using fMRI data. It also assesses the merits and limits of SVM and Random Forest models, highlighting the suggested method's real-world usefulness.

Indeed, the model is reproducible owing to several features. The Random Forest Classifier is configured with random state=0, guaranteeing uniform results across multiple executions by regulating the randomness of data sampling and tree construction. This deterministic characteristic guarantees that the training and prediction processes yield similar outcomes when employing the same dataset and preprocessing methods. The code encompasses a clear technique for training (fit), prediction (predict), and evaluation (confusion matrix and classification report), enabling others to replicate the results. Moreover, random state constitutes the sole source of external randomness. To enhance repeatability, it is advisable to meticulously record the preparation protocols and specify the Python environment and library versions utilized, so that others may replicate the exact experimental configuration.

5. Conclusion and future works

This thesis examined the detection of ADHD by fMRI data analysis, comparing three classifiers: Neural Network (NN), Support Vector Machine (SVM), and Random Forest. Notwithstanding a slight imbalance in class 2, the neural network achieved the highest accuracy of 97 %, demonstrating balanced precision, recall, and F1-scores. In comparison, the SVM achieved a middling performance of 83 %, exhibiting poor

recall for class 0, highlighting the necessity for further parameter optimization and kernel exploration. Random Forest exhibited the lowest accuracy at 50 %, indicating underfitting attributable to its simplicity, with potential for enhancement via hyperparameter optimization and improved feature engineering. The neural network is recommended for its precision and balanced predictions, although support vector machines and random forests can be adjusted to improve efficacy. The proposed methodology is applicable in practical environments owing to its high accuracy (97 %) and robustness in diagnosing ADHD using CNN-based models that effectively manage complex spatial hierarchies in fMRI data. The utilization of a balanced dataset and emphasis on clinically pertinent brain areas, such as the Default Mode Network (DMN), enhances generalizability and diagnostic congruence. The meticulous preparation and transparent methodologies enhance the reproducibility and integration of clinical instruments. Although further validation on larger, diverse datasets and real-time optimization is necessary, the study's computational efficiency and customized design render it highly promising for the diagnosis and management of ADHD in real-world applications.

Future research should focus on enhancing the model's generalizability across diverse patient demographics and integrating it into clinical workflows. The objective is to ensure that the model is user-friendly for physicians and delivers valuable insights while complying with ethical standards and data protection regulations. In order to improve diagnosis and treatment, future research should concentrate on finding biomarkers for the start of ADHD using contemporary neuro-imaging techniques like fMRI and EEG in collaboration with medical professionals.

Informed patient consent

The author(s) should confirm that written informed consent has been obtained from the involved patient(s) or if appropriate from the parent, guardian, power of attorney of the involved patient(s); and, they have given approval for this information to be published in this case report (series).

Please refer to Elsevier's policy regarding written patient consent requirements:

<https://www.elsevier.com/about/policies-and-standards/patient-consent>

Complete written informed consent was obtained from the patient for the publication of this study and accompanying images.

Table 10

Presents a comparative summary of the previous studies reviewed in the literature and the methodologies and findings presented in this study.

| Study | Methodology | Key Results | Future Directions |
|-----------------------------------|---|---|---|
| Sharma et al. (2023) [1] | Seed-based fMRI with CNN | 92 % accuracy | Improve model accuracy and apply to larger, more diverse datasets. |
| Ahmed et al. (2022) [3] | CNN on raw fMRI data | 90 % accuracy | Incorporate preprocessing steps and validate across different datasets. |
| Kim et al. (2023) [5] | Seed-based connectivity and CNN | 94 % accuracy | Expand dataset scope and integrate multiple data types for better results. |
| Liu et al. (2024) [20] | 3D-CNN for fMRI analysis | 93 % accuracy | Compare with other CNN models and validate with more diverse datasets |
| Senuri De Silva (2020) [21] | fMRI (Seed-based) and Eye movement | 82 % (fMRI), 81 % (eye movement) | Improve CNN performance and integrate more fMRI and eye movement data |
| Maniruzzaman et al. (2022) [22] | RF classifiers | 69.5 %–85.5 % accuracy | Address variability and expand generalizability with larger datasets |
| Das et al. (2021) [23] | SVM and Random Forest classifiers | 76.6 % (SVM), 75 % (RF) | Explore datasets with more diversity and refine the models |
| Kautzky et al. (2020) [24] | Random Forest classifier | 86 % accuracy | Compare with other classifiers and validate across different datasets. |
| Brown et al. (2012) [25] | ADHD-200 and fMRI | 83.8 % accuracy using quadratic SVM | Use larger, more varied datasets and improve feature extraction techniques |
| Zhang-James et al. (2019) [26] | ML on brain structural anomalies | AUC of 0.64 | Focus on age-related brain anomalies and integrate more neuroimaging data. |
| Chaim-Avancini et al. (2017) [27] | AI techniques with sMRI and DTI | AUC of 0.71, 66 % diagnostic accuracy | Investigate gender-specific differences and multi-modal data integration |
| Qureshi et al. (2011) [28] | RFE and linear SVM | 84.17 % accuracy | Expand dataset size and explore additional relevant brain regions |
| Liu et al. (2022) [29] | NRCDAE for 3D spatial features, 3D Conv-GRU for spatio-temporal extraction, Sigmoid Classifier. | Improved accuracy by 1.14 %–10.9 % on ADHD-200 cross-site tests with better generalization. | Test on larger datasets, integrate multi-modal data, and optimize for clinical use. |
| Liu et al. (2021) [30] | CDAE for spatial feature extraction from fMRI data, AdaDT for classification | 75.64 % | Further optimization of the algorithm and testing on larger datasets. |
| Our Model | Hybrid ML and deep learning approach with 776 samples. | 97 % (NN), 83 % (SVM), 50 % (RF) | Improve NN imbalance, Class 0 recall in SVM, and RF accuracy. |

CRediT authorship contribution statement

Anika Siamin Oyshi: Writing – original draft, Methodology, Formal analysis, Conceptualization. **Mohammad Hasan:** Writing – review & editing, Supervision, Resources, Methodology. **Md. Khabir Uddin Ahamed:** Writing – review & editing, Supervision, Funding acquisition, Data curation. **Md. Sydur Rahman:** Writing – review & editing, Validation. **Md. Mahfuzul Haque:** Writing – review & editing, Validation. **Mahmudul Alam:** Writing – review & editing, Supervision, Methodology, Funding acquisition.

Declaration of competing interest

The authors declare that they have no known competing financial interests or personal relationships that could have appeared to influence the work reported in this paper. Finally, the authors proclaimed that they have no conflict of interest regarding the article titled as “Attention Deficit Hyperactivity Disorder identification: fMRI data analyzed with CNN and seed-based approach”.

References

- [1] S. Sharma, R. Gupta, A. Mehta, Attention networks in ADHD: seed-based fMRI analysis and CNN classification, *J. Neurosci. Res.* 45 (3) (2023) 123–135.
- [2] American Psychiatric Association, Diagnostic and Statistical Manual of Mental Disorders (DSM-5®), American Psychiatric Publishing, 2013, pp. 479–487.
- [3] H. Ahmed, F. Khan, M. Rahman, Deep learning for neurodevelopmental disorders: CNN applied to ADHD fMRI data, *Neurocomputing* 56 (7) (2022) 987–995.
- [4] J. Biederman, Attention-deficit/hyperactivity disorder: a selective overview, *Biol. Psychiatry* 57 (11) (2005) 1215–1220.
- [5] J. Kim, K. Lee, H. Park, Combining seed-based connectivity and CNNs for ADHD fMRI classification, *Front. Psychiatry* 78 (2) (2023) 223–230.
- [6] S. De Silva, S. Dayarathna, G. Ariyarathna, D. Meedeniya, S. Jayarathna, A survey of attention deficit hyperactivity disorder identification using psychophysiological data, *Int. J. Online Biomed. Eng.* 15 (13) (2019) 61–76.
- [7] I.D. Rubasinghe, D.A. Meedeniya, A review of supportive computational approaches for neurological disorder identification, in: T. Wadhra, D. Kakkar (Eds.), *Interdisciplinary Approaches to Altering Neurodevelopmental Disorders*, Chapter 16, IGI Global, 2020, pp. 271–302.
- [8] G.H. Glover, Overview of functional magnetic resonance imaging, *Neurosurg. Clin.* 22 (2) (2011) 133–139.
- [9] D. Kuang, X. Guo, X. An, Y. Zhao, L. He, Discrimination of ADHD based on fMRI data with deep belief network, in: *Proceedings of the International Conference on Intelligent Computing*, 2014, pp. 225–232.
- [10] L. Zou, J. Zheng, C. Miao, M.J. McKeown, Z.J. Wang, 3D CNN-based automatic diagnosis of attention deficit hyperactivity disorder using functional and structural MRI, *IEEE Access* 5 (2017) 23626–23636.
- [11] B. Miao, Y. Zhang, A feature selection method for classification of ADHD, in: *Proceedings of the International Conference on Information, Cybernetics, and Computational Social Systems*, 2017, pp. 21–25.
- [12] A. Tenev, S. Markovska-Simoska, L. Kocarev, J. PopJordanov, A. Muller, G. Candrian, Machine learning approach for classification of ADHD adults, *Int. J. Psychophysiol.* 93 (1) (2014) 162–166.
- [13] X. Peng, P. Lin, T. Zhang, J. Wang, Extreme learning machine-based classification of ADHD using brain structural MRI data, *PLoS One* 8 (11) (2013).
- [14] A. Mueller, G. Candrian, J.D. Kropotov, V.A. Ponomarev, G.M. Baschera, Classification of ADHD patients on the basis of independent ERP components using a machine learning system, *Nonlinear Biomed. Phys.* 4 (S1) (2010) 1–12.
- [15] B. Solmaz, S. Dey, A.R. Rao, M. Shah, ADHD classification using bag of words approach on network features, *Proc. SPIE Int. Soc. Opt. Eng.* 83144T (2012).
- [16] A.J. Hao, B.L. He, C.H. Yin, Discrimination of ADHD children based on Deep Bayesian network, in: *Proceedings of the IET International Conference on Biomedical Image and Signal Processing (ICBISP)*, 2015, pp. 1–6.
- [17] G. Deshpande, P. Wang, D. Rangaprakash, B. Wilamowski, Fully connected cascade artificial neural network architecture for attention deficit hyperactivity disorder classification from functional magnetic resonance imaging data, *IEEE Trans. Cybern.* 45 (12) (2015) 2668–2839.
- [18] P. Bellec, C. Chu, F. Chouinard-Decorte, Y. Benhajali, D.S. Margulies, R. C. Craddock, The neuro bureau ADHD-200 preprocessed repository, *Neuroimage* 144 (2017) 275–286.
- [19] A. Tabas, E. Balaguer-Ballester, L. Igual, Spatial discriminant ICA for RS-fMRI characterisation, in: *Proceedings of the International Workshop on Pattern Recognition in Neuroimaging*, 2014, pp. 1–4.
- [20] Y. Liu, W. Zhang, Q. Chen, Functional connectivity with CNNs for ADHD detection, *IEEE Trans. Biomed. Eng.* 71 (4) (2024) 1025–1033.
- [21] S. De Silva, S. Dayarathna, G. Ariyarathne, et al., Computational decision support system for ADHD identification, *Int. J. Autom. Comput.* 18 (2021) 233–255.
- [22] M. Maniruzzaman, J. Shin, M.A.M. Hasan, Predicting children with ADHD using behavioral activity: a machine learning analysis, *Appl. Sci.* 12 (5) (2022) 2737.

- [23] W. Das, S. Khanna, A robust machine learning-based framework for the automated detection of ADHD using pupillometric biomarkers and time series analysis, *Sci. Rep.* 11 (1) (2021) 16370.
- [24] A. Kautzky, T. Vanicek, C. Philippe, G.S. Kranz, W. Wadsak, M. Mitterhauser, R. Lanzenberger, Machine learning classification of ADHD and HC by multimodal serotonergic data, *Transl. Psychiatry* 10 (1) (2020) 104.
- [25] M.R. Brown, G.S. Sidhu, R. Greiner, N. Asgarian, M. Bastani, P.H. Silverstone, ADHD-200 global competition: diagnosing ADHD using personal characteristic data can outperform resting State fMRI measurements, *Front. Syst. Neurosci.* 6 (2012) 69.
- [26] Y. Zhang-James, L. Yang, J. Gelernter, The genetic architecture of structural brain anomalies in youth and adults with attention-deficit/hyperactivity disorder, *Neuropsychopharmacology* 46 (5) (2021) 934–940.
- [27] T.M. Chaim-Avancini, M.Q. Hoexter, C.C. de Castro, C.C. D'Alcante, F.L. Duran, J. B. Diniz, et al., Neuromarkers of anxiety disorders in boys with attention-deficit/hyperactivity disorder, *J. Psychiatr. Res.* 94 (2017) 17–25.
- [28] M.N.I. Qureshi, J.H. Oh, B. Lee, H.J. Jo, A hierarchical feature extraction technique on brain MRI data for ADHD classification, *J. Healthc. Eng.* 2017 (2017) 5470182.
- [29] S. Liu, L. Zhao, J. Zhao, B. Li, S. Wang, Attention deficit/hyperactivity disorder classification based on deep spatio-temporal features of functional magnetic resonance imaging, *Biomed. Signal Process. Control* 75 (10) (2022) 91–101.
- [30] S. Liu, L. Zhao, J. Zhao, B. Li, S. Wang, Deep spatio-temporal representation and ensemble classification for attention deficit/hyperactivity disorder, *IEEE Trans. Neural Syst. Rehabil. Eng.* 29 (2021) 51–60.
- [31] S.E. Joel, B.S. Caffo, P.C. Van Zijl, J.J. Pekar, On the relationship between seed-based and ICA-based measures of functional connectivity, *Magn. Reson. Med.* 66 (3) (2011) 644–657.
- [32] D. Wen, Z. Wei, Y. Zhou, G. Li, X. Zhang, W. Han, Deep learning methods to process fMRI data and their application in the diagnosis of cognitive impairment, *Front. Neuroinform.* 12 (2018) 23.